Bite force-gape curves and passive tension costs in *Macaca mulatta*

Stephanie L. Canington[1,*], Carla Escabi[2], Michael L. Platt[2,3,4], Timothy A. Machado[2,5], Jose Iriarte-Diaz[6], and Myra F. Laird[1]

[1]Dept. of Basic and Translational Sciences, University of Pennsylvania School of Dental Medicine, Philadelphia, PA
[2]Dept. of Neuroscience, Perelman School of Medicine, University of Pennsylvania, Philadelphia, PA
[3]Dept. of Psychology, School of Arts and Sciences, University of Pennsylvania, Philadelphia, PA
[4]Marketing Dept., Wharton School of Business, University of Pennsylvania, Philadelphia, PA
[5]Howard Hughes Medical Institute
[6]Dept. of Biology, University of the South, Sewanee, TN

[*]Author for correspondence: steph.canington@gmail.com

ABSTRACT

Passive forces generated by the jaw adductor muscles and their connective tissues are thought to play a protective role in the feeding system by limiting gape to avoid hyperextension and minimize distractive forces at the temporomandibular joint. However, passive muscle forces have only been measured in individual jaw adductors of two non-primate mammals, and it is unknown how these forces translate to bite force at the occlusal surface and affect gape behaviors. We measured *in vivo* passive bite forces in eight adult *Macaca mulatta* at anterior (I_1) and posterior (M_1) bite points across linear gapes ranging from 15-50 mm. Active bite force data were collected at the anterior bite point from two of these macaques (one male; one female) using a custom-built bite force transducer across linear gapes ranging from 10-60 mm. We demonstrate that *M. mulatta* passive bite forces increase with gape and vary by bite point with forces larger at M_1 compared to I_1 for both linear and angular gapes. Our experimental data and Hill-type muscle models of both active and passive forces suggest that passive bite

Journal of Experimental Biology • Accepted manuscript

forces are absolutely and relatively small at the occlusal surface in macaques and play a minimal role in constraining gape. These are the first empirical data on bite force passive tension in primates, and the first data to suggest that the macaque jaw adductor muscles exhibit unusually high compliance potentially relating to selection for large gape behaviors.

Summary Statement

This study compares *in vivo* passive and active bite forces at the occlusal surface in *Macaca mulatta* and discusses implications for bite force-gape tradeoffs and feeding system muscle models.

Keywords: Muscle, feeding, mastication, primate, dental

INTRODUCTION

Bite force is a product of integrated neural signaling, skeletal biomechanics, and muscle physiology. In mammals, bite force is primarily generated by the three major jaw adductor muscles: the masseter, the medial pterygoid, and the temporalis. The total force generated by each of these muscles is the result of both active forces produced by the cross-bridging cycles within sarcomeres (Gordon et al., 1966) and passive tensile forces generated by connective tissue elements (Purslow, 2020), intracellular proteins such as titin (Labeit and Kolmerer, 1995), and the intermediate filament system (Lazarides, 1980). Contractile properties at the level of the sarcomere, the smallest functional contractile unit, as well as the whole muscle (Winters et al., 2011), can be described as a length-tension curve–where force increases until the sarcomere or muscle reaches an optimal point of stretch ($\hat{L}_{f,0}$). If stretched beyond this point, the active force decreases and the passive force increases (**Fig. 1**). Length-tension curves and the role of passive tension have primarily been studied in isolated muscle preparations (e.g., Davis et al., 2003). However, applying these findings to broader functional units, such as the jaw or leg, is challenging because the muscles are a part of complex, integrated systems.

Passive tension is thought to contribute to the mammalian feeding system in several ways. Jaw adductor passive tension was initially proposed to help maintain a resting closed to slightly open jaw position (Yemm, 1976; Rugh et al., 1980; Miller, 1991), but Langenbach and Hannam (1999) suggest both passive and active tension help to maintain jaw position. In the locomotor system, passive tension provides elastic energy storage in muscles such as the gastrocnemius contributing to energy efficiency during locomotion (Biewener, 1998; Ettema, 1996). However, energy costs of the feeding system are small (Laird et al., 2016; van Casteren et al., 2022; Wall et al., 2023), as is the likely importance of passive tension in energy storage for the jaw (Ross and Iriarte-Diaz, 2012). Instead, passive tension is thought to play a protective role in the feeding system by limiting gape to avoid hyperextension, sudden lengthening perturbations, and by minimizing distractive forces at the temporomandibular joint (TMJ; Iriarte-Diaz et al., in review). This protective mechanism has been demonstrated by Horner and colleagues (2024), who show the medial gastrocnemius of rats increases in passive stiffness as the operating length of the muscle shortens, likely limiting the force the animal produces during locomotion. In cercopithecoid primates, passive tension safeguards against TMJ displacement during wide-gape behaviors, including displays, prey capture, and food ingestion. For example, wide-gaped canine display in species such as macaques relate to inter-male aggression and an increased capacity for adductor muscle stretch (Plavcan and van Schaik, 1992; Taylor et al., 2024).

There are few assessments of both active and passive tension in the mammalian feeding muscles. Both active and passive tension were modeled in gouging marmosets and non-gouging tamarins using passive tensions data based on the tibialis anterior of a rabbit, and tamarins had larger passive forces at wide gapes (Eng et al., 2009). Anapol and Herring (1989) report active and passive tension in the masseter and digastric muscles of miniature pigs using nerve cuff stimulation. They found that masseter passive tension costs began to increase prior to the gape associated with optimal force production. Similar results were noted in the masticatory muscles of opossums, which have a larger relative maximum gape (Thexton and Hiiemae, 1975), as well as in rats, where the superficial masseter is proposed to operate at both long and likely unstable lengths while biting mechanically hard foods (Konow et al., 2025). However, more

recent analyses of active and passive tension measured in isolated limb muscles suggest that passive tension is dependent upon the connective tissue of the individual muscle and does not consistently scale with active tension (Winters et al., 2011; Ward et al., 2020; Lieber et al., 2025).

The effects of jaw adductor active and passive tension on bite force at the occlusal surface are of interest for musculoskeletal models of the feeding system. Hill-type muscle models use computational approaches to functional systems that incorporate bony geometry with muscle properties, including muscle architecture measures of fiber length, pinnation angle, and passive tension. While these models are commonly used for the locomotor system (e.g., Hill, 1938, 1950; Anderson and Pandy, 2003; Thelen, 2003; Delp et al., 2007; Peterson et al., 2011; Biewener et al., 2014), such models have only recently been applied to the feeding system (Iriarte-Diaz et al., 2017, in review; Laird et al., 2024). Muscle models of bite force were compared to *in vivo* bite forces from two strepsirrhine primates, *Eulemur* and *Varecia*, and modeled passive components had little to no effect on predicting bite force (Laird et al., 2024). However, it is unknown how modeled and *in vivo* occlusal passive forces compare in primates.

We compare total and passive bite forces at the occlusal surface of rhesus macaques (*Macaca mulatta*) and test the effects of passive tension on muscle models of the feeding system. To estimate the contribution of both active and passive components of muscle force to bite force, we measured bite forces from awake and sedated animals, respectively. Bite forces obtained from sedated animals represent only the passive bite forces. Bite forces recorded from awake animals represent the total bite forces, which combine both passive and active muscle force contributions. Macaques are an ideal model organism for comparing jaw adductor active and passive muscle force as they use both high bite force and large gapes to orally process foods, engage in aggressive or defensive exchanges, and for social or manipulative purposes (e.g., Corlett and Lucas, 1990; Hylander, 2013; Panagiotopoulou et al., 2023). Bite forces in macaques are well studied, with estimates derived from numerous methods including *in vivo*, muscle, tooth mark, and simulation approaches (Laird et al., 2025). Previous *in vivo* approaches to bite force in macaques report a range of 92.18–101.99 N on the incisors and an average of 235 N (maximum 333 N) on the molars using a force transducer (Hylander, 1979).

Dechow and Carlson (1990) used unilateral muscle stimulation to record a mean range of 133.1–151.1 N on the incisors and 286.2–369.3 N on the molars in a sample of 96 adult *Macaca mulatta*. However, there are no published *in vivo* passive bite force values for the primate feeding system, with models including passive muscle forces that have been estimated either using data from other animals (Thexton and Hiiemae, 1975; Anapol and Herring, 1989; van Eijden et al., 2002) or from muscles outside of the feeding system (e.g., rabbit tibialis anterior; Davis et al., 2003). We address three questions:

Question 1: How do passive bite forces relate to gape and vary across the toothrow?

As the jaw is gaped and adductor muscles stretched, passive muscle and bite forces are expected to increase exponentially. Passive bite forces are expected to vary along the toothrow such that posterior bite points are associated with higher bite force values, reflecting the proximity of the bite point to the TMJ (Greaves, 1978).

Question 2: How do passive bite forces relate to peak active bite force and maximum gape?

Masticatory muscle passive tension data from minipigs suggest passive tension costs rise prior to the gape associated with peak bite force, and passive tension values exceed active tension values at or around maximum gape. This serves to safeguard against jaw displacement at the expense of bite force production (Thexton and Hiiemae, 1975; Anapol and Herring, 1989). We expect macaques to show a similar pattern with passive bite force values rising prior to peak active bite force and surpassing active tension values near maximum gape.

Question 3: How do passive forces influence Hill-type muscle model predictions of bite force and operating range?

Models of the primate feeding muscles either do not include passive muscle forces or estimate passive tension from other animals and/or muscles (e.g., Thexton and Hiiemae, 1975; Anapol and Herring, 1989; Davis et al., 2003). We expect the inclusion of passive muscle force

estimates from *in vivo* passive bite force data in Hill-type models of the feeding system to produce similar bite force and operating range estimates as models without passive muscle force estimates (Laird et al., 2024). However, bite force and operating range estimates are expected to be different from models using passive tension estimates from other animals and/or muscles.

MATERIALS AND METHODS

Passive and active tension data

A total of 74 measures of *in vivo* passive bite force were collected from eight *Macaca mulatta* (5 females, 3 males) adults at linear gapes ranging from 15 to 50 mm. Total bite force-gape data were collected from two of the macaques included in the passive bite force sample (Hk-male and Ll-female). Active bite force-gape data were not collected for the other six macaques in the passive sample due to animal training availability. All data were collected at the University of Pennsylvania and approved by the University of Pennsylvania Institutional Animal Care and Use Committee (#805870).

Bite force data were recorded using a custom-built bite force transducer based on a model described by Herrel and colleagues (2001; 2004; 2005) and others (e.g. Verwaijen et al., 2002; Aguirre et al., 2003; Laird et al., 2023a; 2024). Two metal plates were fixed to a compressive piezoelectric load cell (Kistler 9203), and the spacing between the plates was changed using an adjustable micrometer (Mitutoyo 152-103). Increased space between the bite plates resulted in a larger linear gape (in mm). Compressive loads were amplified (Kistler 5995A), passed through an analog-to-digital converter (Adafruit Industries ADS1115), and logged on a Raspberry Pi 4 Model B using custom Python code. Athletic tape was wrapped around the metal plates to protect the animal's teeth. Amplified output loads were converted to Newtons of force by conducting calibration experiments using a series of 100, 200, and 500g weights that were statically placed on the bite plates, including the athletic tape, at 10-, 15-, and 20-mm linear gape determined by spacing between the bite plates. There were no

significant differences in the forces between gapes in the calibration experiments, and we used a standard correction factor (Laird et al., 2023a; 2024).

Passive bite force data were collected using this bite force transducer during semi-annual veterinary sedations conducted by University Laboratory Animal Resources veterinarians and veterinary technicians in February 2024 and 2025. Sedation was achieved using a combination of 4 mg/kg of ketamine and 0.025 mg/kg of dexmedetomidine, and all animals had a negative palpebral reflex and relaxed jaw tone before passive bite force data collection. While the animal was sedated, the bite plates of the transducer were successively spaced between 15 and 50 mm linear gape in 5 mm increments and positioned between the central incisors and between the right first molars. The bite plates were held between the teeth until the force plateaued, the bite plates were removed, and the jaw was allowed to close between each gape increment and between bite positions on the incisors and molars. For large linear gapes, the jaw was also gently translated anteriorly. Linear gapes smaller than 15 mm did not register measurable bite forces using this setup and were not included in the analyses. While sedated, each animal was weighed on a digital scale, and a series morphological measurements were recorded on the face using sliding calipers: jaw length (the distance between condylion laterale to infradentale), facial width (the distance between the left and right lateral canthus of the eyes), maximum gape (measured between the central incisors), and, if present, the amount of incisor overlap or spacing (following Hylander, 2013; **Table 1**).

Total bite force-gape data were collected for two of the macaques at the incisors (HK - male; LL - female) over a period of eight months. A total of 419 voluntary bites (HK - 311; LL - 108) were collected from these animals between normal meal times, and neither animal was water or food restricted. Bites were recorded in 5 mm increments at linear gapes ranging from 10 mm to 55 mm for LL and between 15 and 60 mm for HK. Both animals received water-diluted apple or grape juice as a reward for biting, which was administered by a plastic cannula taped to the underside of the top bite plate. Bites were loosely threshold trained, meaning that the animal had to elicit stronger and stronger bites to receive reward, and reward was withheld for bites with lower force (described in Laird et al., 2023a). Only the maximum forces recorded at each gape for each animal were included in the analyses. Maximum linear gape at the central

incisors measured under sedation was 63.76 mm for animal HK and 54.18 mm for LL. The largest linear gape for which active bites were recorded was 60 mm for animal HK and 55 mm for LL, suggesting that active force was measured at or near their maximum linear gapes. Active bite forces were isolated by subtracting the passive bite force data from the total bite force data.

Behavior data

Bite force data in primates are best contextualized using multiple sources (Laird et al., 2025), and we supplemented the transducer forces for monkeys HK and LL using shell fracture properties of two nuts. Both animals were provided with English walnuts and Brazil nuts in the shell (www.nuts.com) and filmed while feeding on these items using a Sony Handycam video camera (HD CRX405). Videos were reviewed to determine the location of fracture (incisors versus postcanine dentition). Force-to-fracture estimates for English walnut (233.39 N) and Brazil nut (614.46 N) shells were collected from the literature (Laird et al., 2023). Dimensions of both nuts were collected using digital calipers (**SOM Tables 1 and 2)**.

Passive and total bite force analyses

Maximum passive and total bite forces within each trial were segmented using the packages 'pracma' (Borchers, 2019), 'quantmod' (Ryan et al., 2020), and 'splitstackshape' (Mahto, 2019) in R (R Core Team, 2025). We analyzed both linear and angular gape, which was calculated using jaw length measurements for each animal. Linear mixed effects models for linear and angular gape were used to test differences in passive tension between I_1 (anterior) and M_1 (posterior) locations on the toothrow and to test whether passive tension differed between males and females. Tests were conducted using the package lme4 (Bates et al., 2015) and post-hoc tests in package emmeans (Lenth, 2023). Models for differences in passive tension at each bite point were constructed with the identification of each animal and sex as random factors, and sex was moved to an explanatory variable to test for differences between males

and females. To determine whether forces at each linear gape were significantly greater than zero, separate models were fit for anterior and posterior measurements with linear gape as a fixed effect and animal and sex as random effects. Estimated marginal means with 95% confidence intervals were used to identify linear gape levels where forces exceeded zero. These tests were only conducted on linear gape as a categorical variable. Significance level was set as 0.05.

Construction of virtual bone and muscle segment models

3D skeletal and muscle data

Muscle segment models were created using PLY mesh skull models downloaded from MorphoSource (Boyer et al., 2016) of an adult male and female *Macaca mulatta* (specimen IDs 000543170 and 000543165, respectively). These 3D meshes were cleaned and oriented such that the Y-axis passes through the left and right temporomandibular joints (TMJs) and the X-axis is parallel to the premolar and molar occlusal plane using Geomagic Wrap 2017 (Geomagic, Morrisville, NC). Full details on the muscle segments are described in Iriarte-Diaz et al. (2017) and Laird et al. (2024). Briefly, the three jaw adductor muscles were modeled using a series of seven equidistant segments aligned between the cranial and mandibular attachments and wrapped to the surface of the model. These 3D muscle models were used to simulate changes in gape by rotating the mandible from 0 to 50 degrees at 5-degree increments. At each gape increment, the mandible was also translated so that the ramus cleared the postglenoid process and that the condyle remained in tangential contact with the glenoid fossa. For each gape, force position and direction were calculated for the virtual muscle segments. Muscle architecture data was obtained from Taylor and colleagues (2018) and shown in **Table 2.**

The 3D model data (cranium, mandible, and virtual muscles) and the muscle architecture data were scaled to match the jaw length of each subject using the measurements recorded from each animal during sedation. For linear variables such as fiber lengths, linear gapes, moment arms, and muscle positions, values were scaled by multiplying the variable by $L_{j,exp}/L_{j,MA}$, where $L_{j,exp}$ and $L_{j,MA}$ are the jaw length of the specific experimental subject and the

jaw length from the muscle architecture data, respectively. PCSA was scaled by multiplying it by $(L_{j,exp}/L_{j,MA})^2$.

Linear gapes were transformed to angular gapes by measuring the linear distance between the upper and lower teeth (I_1 for anterior bites and M_1 for posterior bites) of the scaled 3D model at different gape angles, and then interpolating the experimental linear gapes.

To compare anterior and posterior bites, bite forces on posterior teeth ($F_{bite,M1}$) were scaled to estimate bite forces on anterior teeth ($F_{bite,I1}$) as:

$$F_{bite,I1} = \frac{F_{bite,M1}\, d_{M1}}{d_{I1}}, \#[1]$$

where d_{I1} and d_{M1} are the perpendicular distances of the first incisor and the first molar from the TMJ axis, respectively, where the TMJ axis is the line connecting the left and right TMJs.

Estimation of muscle and bite forces

Virtual 3D muscle models were created for one female and one male macaque. We created three different 3D models for each sex based on the active tension data collected from animals HK and LL: (1) a model without including passive tension, (2) a model similar to past approaches that optimizes both active and passive parameters to best fit the experimental bite force data, and (3) a model with individual-specific *in vivo* passive bite forces at the occlusal surface reported here.

Bite force at a particular bite point was estimated from the three jaw adductors, masseter, temporalis, and medial pterygoid, by first estimating force for each muscle segment and then summing across the muscles.

Bite force produced by individual muscle segments for a given gape was estimated using the equation:

$$F_{bite\ (gape)} = \frac{2\, F_{m\ (gape)}\, d_m}{d_{bite}}, \#[2]$$

where $F_{m\,(gape)}$ is the maximum force generated by an individual muscle segment at a given gape, d_m is the moment arm (perpendicular distance of the TMJ axis) of the segment of muscle, d_{bite} is the moment arm of the bite point, and is multiplied by two to simulate the effect of both muscle sides.

$F_{m\,(gape)}$ was calculated using a Hill-type model as:

$$F_{m\,(gape)} = F_{max}\left(\hat{f}_a + \hat{f}_p\right) cos\ \alpha_{(gape)}\ ,\#[3]$$

where $\hat{f}_a$ and $\hat{f}_p$ are the normalized active and passive force-length relationships (**Fig. 1**), $\alpha_{(gape)}$ is the pennation angle for a given gape, and F_{max} is the maximum tetanic force that the muscle segment can generate, calculated as:

$$F_{max} = \frac{\sigma\ PCSA}{n_s}\ ,\#[4]$$

where σ represents the specific tension of skeletal muscle (estimated as ~30 N/cm^2 for homogeneously IIM muscle), PCSA is the physiological cross-sectional area of the muscle (in cm^2; see Laird et al., 2024 and Taylor et al., 2025), and n_s indicates the number of segments per muscle.

The normalized active force-length curve was given by the equation (equation HH in Rockenfeller and Günther, 2017):

$$\hat{f}_a = e^{-\left(\frac{\left(\hat{L}_{f\,(gape)} - \Delta L_a\right) - 1}{0.41}\right)^2}\ ,\#[5]$$

and the normalized passive force-length curve was defined by the equation (Dick et al., 2017):

$$\hat{f}_p = 2.64\left(\hat{L}_{f\,(gape)} - \Delta L_p\right)^2 - 5.30\left(\hat{L}_{f\,(gape)} - \Delta L_p\right) + 2.66 \quad for\ \hat{L}_{f\,(gape)} > 1\ ,\#[6]$$

$$\hat{f}_p = 0 \quad for\ \hat{L}_{f\ (gape)} \leq 1, \#[7]$$

where $\hat{L}_{f\ (gape)}$ is the muscle fiber length for a given gape normalized to $L_{f,occ}$, the fiber length at occlusion, and ΔL_a and ΔL_p are active and passive offset parameters, respectively, which are optimized for each subject (see *Optimization of muscle parameters* below). ΔL_a represents how much a muscle fiber has to be stretched from occlusion to reach its optimal length, while ΔL_p represents the normalized slack length–how much the fiber has to be stretched to start generating passive force. $\hat{L}_{f\ (gape)}$ was calculated by the equation (Laird et al., 2024):

$$\hat{L}_{f\ (gape)} = \sqrt{\frac{\left(L_{f,occ}\ sin\ \alpha_{occ}\right)^2 + \left(L_{f,occ}\ cos\ \alpha_{occ} + \Delta L_{s\ (gape)}\right)^2}{L_{f,occ}^2}}, \#[8]$$

where α_{occ} is the pennation angle at occlusion, and $\Delta L_{s\ (gape)}$ is the difference in the length of the muscle segment for a given gape with respect to the segment length at occlusion, measured directly from the 3D muscle models. Equation 8 assumes that muscle fibers are parallel, coplanar, and of equal width (Azizi and Deslauriers, 2014; Dick and Wakeling, 2018) and (2) as the length of the muscle changes, pinnation angle varies while muscle thickness does not (see Laird et al., 2024).

Optimization of muscle parameters

Our muscle model requires the estimation of the active and passive offset parameters (ΔL_a and ΔL_p) as well as of active and passive correction factors (cf_a and cf_p), which affect the magnitude of the predicted bite force, but does not change the shape of the bite force-gape relationship. All parameters were estimated using the MATLAB “lsqcurvefit” function with the

Levenberg-Marquardt algorithm, which searches for the best combination of parameters that minimizes the least-square differences between the predicted bite force values from the model and the *in vivo* data at different gapes.

For all individuals, we first estimated the passive parameters (ΔL_p and cf_p) alone using the experimentally collected bite force data on anesthetized animals, which was used to determine the passive component of the bite force-gape relationship.

For the two individuals (HK and LL) with total bite force data collected experimentally, we tested three muscle models with different optimization conditions. The first model, `Passive First', uses the ΔL_p and cf_p passive parameters calculated above from the passive bite force data, and then only optimizes the active parameters (ΔL_a and cf_a) that best fit the total bite force data. In this model, the cf_a and cf_p parameters can have different values. The second model, 'Total Force', optimized both the active parameters (ΔL_a and cf_a) and the passive parameters (ΔL_p and cf_p) together to best fit the experimental total bite force data only. In this model, the experimental passive bite force data is not used, and the cf_a and cf_p parameters are the same. The third model, 'Total Force Constrained', optimizes both active and passive parameters to best fit the experimental total bite force data, but constrained so that the ΔL_a and ΔL_p parameters are the same, and the cf_a and cf_p parameters are the same.

RESULTS

Question 1: Passive bite force varies with gape and location on the dentition.

Passive bite forces at both anterior and posterior bite points were significantly positively correlated with both linear and angular gape such that higher passive bite forces were recorded at larger gapes ($p < 0.01$; **Fig. 2**; **SOM Table 3**; **Table 3**). Linear gapes below 15 mm did not register passive bite forces. As expected, passive bite forces differed between anterior and posterior bite points. A bite point at M_1 was associated with passive bite forces that were 2.6 times larger than those on the anterior dentition ($p < 0.01$). On the anterior dentition for linear gapes, females have significantly higher passive bite forces compared to

males (p = 0.03), but there are no significant differences between the sexes in passive bite forces at M_1 for linear gape or for angular gape at the incisors or M_1 (**SOM Table 3**; **SOM Fig 1** and **2**).

Question 2: Passive bite forces vary in relation to peak bite force and maximum gape.

Total bite forces were measured for one male (HK) and one female (LL) macaque. The maximum bite force for LL was 229.69 N measured at 25 mm linear gape, whereas the maximum for HK was 319.14 N recorded at 30 mm linear gape, which is the highest reported *in vivo* incisor force from a macaque (**Table 4**; Laird et al., 2025). Shelled nut fracture was used as a secondary measure of assessing bite force (**SOM Table 2**). Macaque LL did not fracture English walnut or Brazil nut shells on the incisors, which is consistent with our transducer data. However, macaque HK fractured both the English walnut and Brazil nut shells using his incisors, which suggests that 319 N is an underestimate of his maximum total bite force.

As expected, total bite forces in both animals increased with larger gapes until reaching their respective maxima at 25 mm (LL) and 30 mm (HK) linear gape, after which bite force decreased with larger gapes (**Fig. 3**; **SOM Fig. 2**). Across all animals, confidence intervals for the relationship between anterior passive bite forces and gape indicate that forces at linear gapes larger than 30 mm were significantly different from zero, and posterior passive bite forces were significantly different from zero for linear gapes larger than 25 mm (**SOM Table 4**). Difference in confidence intervals for males and females could not be tested due to low sample sizes. This suggests passive bite forces significantly differ from zero around maximum gape; however, total forces in both animals were substantially larger than passive bite forces at all gapes, including at maximum gape.

Question* 3: *How do passive muscle forces influence Hill-type muscle model predictions of bite force and operating range?

Optimized passive parameters based on the passive bite force data show that the ΔL_p ranges from 0.25 to 0.43, but the correction factors cf_p indicate that passive bite forces are largely overestimated by the model ($cf_p < 0.1$; **SOM Table 5**; **SOM Fig. 2**). For the two individuals with total bite force data, two of the muscle models fit the experimental data reasonably well ($R^2 > 0.58$; models `Passive First' and `Total Force') while one model overestimated bite forces at large gapes ($R^2 < 0.46$; `Total Force Constrained'; **Fig. 4**). Models `Passive First' and `Total Force' have similar active offset parameters $\Delta L_a$ between 0.47 and 0.52, but they differ in their passive offset parameters (**Table 5**). Model `Passive First' has ΔL_p values between 0.25 and 0.33, indicating that the passive muscle forces start developing before the muscle fibers reach their optimal length ($\Delta L_p < \Delta L_a$), but increase very slowly with gape. In contrast, the `Total Force' model has ΔL_p values well above the optimal muscle length ($\Delta L_p > \Delta L_a$). This results in a model that effectively does not have a passive bite force component within the range of gapes measured. In other words, this model represents a model with only an active force component (**Fig. 4**). Finally, the `Total Force Constrained' model also has similar $\Delta L_a$ values to the `Passive First' and the `Total Force' models, but the ΔL_p is constrained to be the same as ΔL_a. In this model, the passive muscle force component starts increasing substantially at around 20-degree gapes, overestimating the measured passive bite force values.

DISCUSSION

Measures of passive muscle force of the mammalian feeding system are limited (but see Thexton and Hiiemae, 1975; Anapol and Herring, 1989; Konow et al., 2025), although the expectation is that passive muscle forces are on par with, or exceed, active force when stretched based on a Hill-Type length-tension model (**Fig. 1**; Hill, 1938, 1950). Here, we tested how *in vivo* passive and total bite forces vary with gape in a primate, the rhesus macaque, and found that passive bite force is substantially lower than active force, even at large gapes. We

acknowledge that our total force sample is limited to two animals, and that the use of sedatives has previously been noted to increase muscle stiffness (e.g., tongue stiffness under general anesthesia, Kappert et al., 2021), potentially affecting the jaw adductors. However, increased muscle stiffness would have limited gape stretch, resulting in higher passive bite force values than what might be expected under other sedation methods. Our passive bite force values may therefore be an upper bound, and are still substantially lower than total bite force values. Further, the role of sedatives, including midazolam and dexmedetomidine, have been linked with increased bite force production through the loss of the proprioceptive function of the periodontal ligament (Sivasubramani et al., 2019), effectively suppressing the body's natural neural feedback loop for risking damage to the system. This study is the first to compare primate *in vivo* passive and active bite forces at the occlusal surface, and we discuss the implications of these data for bite force-gape tradeoffs and muscle models of the feeding system.

To contextualize the total bite force data, we compare our data to the extensive literature on bite forces in macaques (reviewed in Laird et al., 2025). We report the highest *in vivo* bite forces for adult male and female macaques measured using a force transducer on the incisors (male: 319.14 N; female: 229.69 N). These values are more than twice the magnitude of previously reported *in vivo* and stimulated incisor forces (Hylander, 1979; Dechow and Carlson, 1990), but smaller than reported incisor force values estimated using food fracture, muscle architecture, and jaw leverage (Hill et al., 1995; Deutsch et al., 2020; Holmes and Taylor, 2023). These data are also consistent with our behavior data, although 319.14 N may be an underestimate of animal Hk's incisor bite force. We compared our maximum gape values to previous studies. All but one of the animals measured here had maximum gapes smaller than the reported male and female ranges of a sample of 50 *M. mulatta* (Hylander, 2013). However, all maximum gapes for the animals in this study were within their respective male and female ranges for a sample of 117 adult rhesus macaques from Cayo Santiago, Puerto Rico (Canington et al., under review).

Primate jaw adductor passive forces are small across the jaw's operational range

Collectively, our results demonstrate that *M. mulatta* passive bite forces across the toothrow increase with gape. This means that as the jaw opens, the jaw adductor muscles are stretched, resulting in the generation of tensile forces from the connective tissue, proteins (e.g., titin), and other structural elements in the absence of active contraction (Gordon et al., 1966; Lazarides, 1980; Labeit and Kolmerer, 1995; Purslow, 2020). As expected, passive bite forces were larger at M_1 compared to the incisors for comparable linear and angular gapes. This difference reflects the shorter moment arm of an M_1 bite point to the TMJ, and the larger amount of gape needed to open the jaw to a particular angle or linear distance at a posterior bite point compared to a bite point at the incisors (Greaves, 1978). Our results also suggest a few differences in passive bite forces between males and females, as the only measure demonstrating significant sexual dimorphism was passive bite force at the incisors across linear gapes (**SOM Table 3**). Muscle architecture data from *M. fascicularis* suggest males have longer jaw adductor fibers compared to females (Terhune et al., 2015), and coupled with males having larger maximum gapes (**Table 1**; Hylander, 2013), this implies that passive bite forces generated by the jaw adductors in males should be lower than females for a given gape. While this pattern held for our incisive measures across linear gapes, our total sample size was small. We expect greater sexual dimorphism in passive bite forces with increased sampling.

Previous studies of passive tension in the feeding system noted that passive forces began to increase prior to peak active force (**Fig. 1**; Thexton and Hiiemae, 1975; Anapol and Herring, 1989; Konow et al., 2025). Our data were consistent with these prior findings. We found that passive bite forces significantly differed from zero around peak total bite force in our two animals (**Figs. 3** and **5**). Our data are also in line with previously published opossum data (Thexton and Hiiemae, 1975), with passive bite forces neither exceeding nor nearing active bite forces, despite recording close to maximum gape. However, the macaque passive forces differed from those of minipigs (Anapol and Herring, 1989), and to a lesser degree rats (Konow et al., 2025), that were more similar to the Hill-type model expectations. The similarity between macaques and opossums is notable as both taxa use large gapes associated with different behaviors. *Didelphis virginiana* is known to hold large gapes for display as part of their fear

responses, but this behavior is rarely accompanied by an attack (McManus, 1970). Holding a wide gape without generating large active bite forces may seemingly benefit from high passive tension, as predicted by a Hill model, which could theoretically stabilize the TMJ, allowing gape to be maintained with low adductor muscle activity. These results are also consistent with modeled passive tension data in gouging marmosets and non-gouging tamarins, as larger modeled passive tension values were reported in non-gouging tamarins (Eng et al., 2009).

Macaques accompany large gapes with aggressive and defensive behaviors involving active bite force generation, such as canine biting (Altmann, 1967; Plavcan and van Schaik, 1992; Highlander, 2013; Terhune et al., 2015). Despite this difference in the use of force at large gapes, both macaques and opossums had similar passive estimates, indicating that passive forces play a minimal role in constraining the TMJ and are minimally influenced by large gape behaviors. It may be the case that anatomical differences between these taxa (e.g., stiffness of connective tissues and mechanical advantage) may elucidate how passive costs are similarly achieved despite behavioral differences.

Despite similarities in findings, there are notable differences in approach between our and these referenced studies. Past studies tested single muscles and estimated active forces using nerve cuff stimulations, and nerve cuffs are unlikely to generate maximum active tension across the entire muscle (Anapol and Herring, 1989). We analyzed both passive and total bite forces at the teeth, which means our estimates included contributions from all of the jaw adductor muscles in their anatomical positions. Functionally heterogeneous muscles, such as the anterior and posterior regions of temporalis, were therefore able to undergo differing amounts of stretch that may have contributed to our low passive muscle forces (Laird et al., 2020; 2023). Passive muscle forces also differ depending on connective tissue and individual muscle structure (Lieber et al., 2025). Thus, measuring passive and total bite forces at the teeth, as opposed to isolated muscles, is inclusive of all jaw adductors within the geometry of the feeding system, which can inform the biological context for these forces. However, additional tests of passive bite force generation are needed across the jaw adductors and between single muscles and the teeth.

Within a single muscle, passive forces provide limits on muscle stretch to avoid structural damage. Passive bite forces are similarly proposed to limit gape and minimize distractive forces at the TMJ in the feeding system, minimizing the risk of structural damage (as seen in the locomotor system, Horner et al., 2024). However, we found that primates do not reach large passive bite forces, even near maximum gape. This suggests that passive forces provide few constraints and protective mechanisms at the TMJ during large gape behaviors in macaques. The bony morphology of the TMJ may instead prevent the jaw adductor muscles from reaching high levels of passive tension (Terhune et al., 2022). However, we caution that this may not be true in all primates. Strepsirrhines have a broad, shallow TMJ with fewer bony constraints compared to the TMJ of an anthropoid primate (Terhune et al., 2022). However, a recent reevaluation of the constrained lever model suggests that no primates have distractive forces at the TMJ at gapes larger than 15 degrees (Iriarte-Diaz et al., in review).

Passive forces play a minor role in Hill-type muscle models of the feeding system

The estimated parameters of the Hill-type muscle models, where passive and active force components were optimized independently (`Passive First'), show that passive forces start increasing on the ascending limb of the length-tension curve, approximately at $0.8\hat{L}_{f,0}$, as it has been observed for jaw adductor muscles in other mammals (Thexton and Hiiemae, 1975; Anapol and Herring, 1989). However, our data shows that passive muscle forces increase very slowly with gape. Our *in vivo* passive bite forces are much lower than predicted by the muscle models (11x lower for HK and 16x lower for LL). A possible explanation for such overestimation could be that the model input parameters overestimate the size of the experimental animals. However, this explanation seems unlikely, considering that the same model underestimates the total bite force in both experimental subjects (by 60% and 27% for HK and LL, respectively). The `Total Force' models were fit using only total bite force data, and were similar to the `Passive First' models (**Fig. 5**), further suggesting that passive components have little impact on the generation of force in the jaw adductor muscles of the rhesus macaque.

These results are drastically different from the bite forces predicted by traditional Hill-type models (`Total Force Constrained'; **Fig. 5**), where passive muscle forces are only present

beyond the optimal muscle length, increasing exponentially so that at 50% muscle stretch, passive tension equals maximum active force (Otten, 1987; Zajac, 1989). This is an unexpected result, considering that passive forces are shown to be larger in whole muscles compared to single muscle fibers or bundles of fibers due to the greater importance of the extracellular matrix (Ward et al., 2020). To be able to compare our data with other muscles and organisms, we calculated the L_{20}, the relative muscle length that develops 20% of the maximal relative muscle force, for the jaw adductor muscles evaluated here, which range between 1.7 and 1.8. This is substantially higher than the range of L_{20} (L_{20} = 1.1) observed for hindlimb muscles in mammals (between 1 and 1.44; Azizi and Roberts, 2010; Horner et al., 2024), and even higher than the average for anurans (L_{20} = 1.5; Azizi and Roberts, 2010). This high muscle compliance observed in anurans has been thought to be necessary for the large joint excursions associated with jumping, as it has been suggested that increased passive muscle stiffness can limit the muscle's range of motion (Brown et al., 1996; Horner et al., 2024). The only data on jaw muscles, to our knowledge, comes from the jaw adductor muscles of anole lizards, with L_{20} ranging from 1.24 to 1.37 (Anderson and Roberts, 2020). Together, these findings demonstrate that macaque jaw adductor muscles exhibit unusually high compliance relative to both limb and jaw muscles of other animals that may relate to selection for large gape behaviors. These data highlight a departure from existing muscle models and present a new framework for comparative analyses of musculoskeletal design.

ACKNOWLEDGEMENTS

Thanks to Penn ULAR veterinarians, technicians, and husbandry staff for animal care. This study was supported by the National Science Foundation's Biological Anthropology directorate BCS-1945771, BCS1944915, BCS-1945283, BCS-1945767, the University of Pennsylvania, NIH R37-MH109728, and by the Appalachian College Association (Semester Professional Leave Fellowship to J.I-D). For the two macaque skulls, the Caribbean Primate Research Center is supported by the University of Puerto Rico and the Office of Research Infrastructure Programs (ORIP) of the National Institute of Health (NIH). The population of Cayo

Santiago was supported by grant number P40OD012217 from the Office of Research Infrastructure Programs (ORIP) of the National Institute of Health (NIH) and the Medical Sciences Campus of the University of Puerto Rico. The content of this publication is solely the responsibility of the authors and does not represent the official views of ORIP or the NIH.

Author contributions

Stephanie L. Canington (scaning@upenn.edu): Conceptualization (equal), Data curation (equal), Formal analysis (equal), Investigation (equal), Methodology (equal), Project administration (equal), Resources (equal), Software (equal), Validation (equal), Visualization (equal), Writing - original draft (equal), & Writing - review and editing (equal);

Carla Escabi (Carla.Escabi@pennmedicine.upenn.edu): Project administration (equal) & Writing - review and editing (equal).

Michael L. Platt (mplatt@pennmedicine.upenn.edu): Funding acquisition (equal), Project administration (equal), Resources (equal), and Writing - review and editing (equal).

Timothy A. Machado (Timothy.Machado@pennmedicine.upenn.edu): Methodology (equal), Software (equal), Writing - review and editing (equal).

Jose Iriarte-Diaz (jairiart@sewanee.edu): Conceptualization (equal), Data curation (equal), Formal analysis (equal), Investigation (equal), Methodology (equal), Project administration (equal), Resources (equal), Software (equal), Validation (equal), Visualization (equal), Writing - original draft (equal), & Writing - review and editing (equal).

Myra F. Laird (mflaird@upenn.edu): Conceptualization (lead), Data curation (equal), Formal analysis (equal), Funding acquisition (equal), Investigation (lead), Methodology (equal), Project administration (equal), Resources (equal), Software (equal), Supervision (lead), Validation (equal), Visualization (equal), Writing - original draft (equal), & Writing - review and editing (equal).

Data availability statement

Original data for this study are available from the corresponding author upon reasonable request.

Funding statement

This study was supported by the National Science Foundation's Biological Anthropology directorate BCS-1945283, the University of Pennsylvania, NIH R37-MH109728, and by the Appalachian College Association (Semester Professional Leave Fellowship to J.I-D).

Conflict of interest disclosure

The authors declare that there is no conflict of interest regarding this publication.

Ethics approval statement

All experiments were reviewed and approved by the University of Pennsylvania Institutional Animal Care and Use Committee #805870.

REFERENCES

Aguirre, L. F., Herrel, A., Van Damme, R., & Matthysen, E. (2003). The implications of food hardness for diet in bats. *Functional Ecology*, 17(2), 201–212.

Altmann, S. A. (1967). The structure of primate social communication. S.A. Altmann (Ed.), Social communication among primates, University of Chicago Press, Chicago, pp. 3325-3362.

Anapol, F., & Herring, S. W. (1989). Length-tension relationships of masseter and digastric muscles of miniature swine during ontogeny. *Journal of Experimental Biology*, 143(1), 1-16.

Anderson, F. C., & Pandy, M. G. (2003). Individual muscle contributions to support in normal walking. *Gait & Posture*, 17(2), 159–169.

Anderson, C. v., & Roberts, T. J. (2019). The need for speed: functional specializations of locomotor and feeding muscles in *Anolis* lizards. *Journal of Experimental Biology*, *223*(2). https://doi.org/10.1242/jeb.213397

Azizi, E., & Deslauriers, A. R. (2014). Regional heterogeneity in muscle fiber strain: The role of fiber architecture. *Frontiers in Physiology*, 5, 103613.

Azizi, E., & Roberts, T. J. (2010). Muscle performance during frog jumping: influence of elasticity on muscle operating lengths. *Proceedings of the Royal Society B: Biological Sciences*, *277*(1687), 1523–1530.

Bates, D., Mächler, M., Bolker, B., & Walker, S. (2015). Fitting Linear Mixed-Effects Models Using lme4. *Journal of Statistical Software, 67*(1), 1–48.

Biewener, A. A. (1998). Muscle-tendon stresses and elastic energy storage during locomotion in the horse. *Comparative Biochemistry and Physiology Part B: Biochemistry and Molecular Biology*, 120(1), 73-87.

Biewener, A. A., Wakeling, J. M., Lee, S. S., & Arnold, A. S. (2014). Validation of Hill-type muscle models in relation to neuromuscular recruitment and force–velocity properties: predicting patterns of in vivo muscle force. *Integrative and Comparative Biology*, 54(6), 1072-1083.

Borchers, M. H. W. (2019). Package 'pracma'. Practical numerical math functions, version, 2(5).

Brown I. E., Cheng E. J.& Loeb G. E. (1999) Measured and modeled properties of mammalian skeletal muscle. II. The effects of stimulus frequency on force–length and force–velocity relationships. *J. Muscle Res. Cell. Motil.* 20, 627–643.

Boyer, D. M., Gunnell, G. F., Kaufman, S., & McGeary, T. M. (2016). Morphosource: archiving and sharing 3-D digital specimen data. The Paleontological Society Papers, 22, 157-181.

Canington S. L., Turcotte, C. M., Hernandez-Janer, E. M., Stock, M. K., Villamil, C. I., Cayo Biobank Research Unit, Montague, M. J., Martinez, M. I., Williams, S. A., Antón, S. C., Higham, J. P., & Laird, M. F. (In review). *Maximum gape in developing* Macaca mulatta.

Chalk-Wilayto, J., Fogaça, M. D., Wright, B. W., van Casteren, A., Fragaszy, D. M., Izar, P., ... & Laird, M. F. (2022). Effects of food material properties and embedded status on food processing efficiency in bearded capuchins. *American Journal of Biological Anthropology*, 178(4), 617-635.

Corlett, R. T., & Lucas, P. W. (1990). Alternative seed-handling strategies in primates: seed-spitting by long-tailed macaques (*Macaca fascicularis*). *Oecologia*, *82*(2), 166-171.

Crompton, A.W., Lieberman, D.E., & Aboelela, S. (2006). Tooth orientation during occlusion and the functional significance of condylar translation in primates and herbivores. In: (pp. 367- M.T. Carrano (Ed.), Amniote Paleobiology. Perspectives on the Evolution of Mammals, Birds, and Reptiles, Univ. of Chicago Press, Chicago, Illinois.

Davis, J., Kaufman, K. R., & Lieber, R. L. (2003). Correlation between active and passive isometric force and intramuscular pressure in the isolated rabbit tibialis anterior muscle. Journal of biomechanics, 36(4), 505-512.

Dechow, P. C., & Carlson, D. S. (1990). Occlusal force and craniofacial biomechanics during growth in rhesus monkeys. American Journal of Physical Anthropology, 83(2), 219-237.

Deutsch, A. R., Dickinson, E., Leonard, K. C., Pastor, F., Muchlinski, M. N., & Hartstone-Rose, A. (2020). Scaling of anatomically derived maximal bite force in primates. *The Anatomical Record*, *303*(7), 2026-2035.

Delp, S. L., Anderson, F. C., Arnold, A. S., Loan, P., Habib, A., John, C. T., Guendelman, E., & Thelen, D. G. (2007). OpenSim: Open-source software to create and analyze dynamic simulations of movement. IEEE Transactions on Biomedical Engineering, 54(11), 1940–1950.

Dick, T. J. M., & Wakeling, J. M. (2018). Geometric models to explore mechanisms of dynamic shape change in skeletal muscle. *Royal Society Open Science*, 5(5), 172371.

Dick, T. J. M., Biewener, A. A., & Wakeling, J. M. (2017). Comparison of human gastrocnemius forces predicted by Hill-type muscle models and estimated from ultrasound images. Journal of Experimental Biology, 220(9), 1643–1653.

Eng, C. M., Ward, S. R., Vinyard, C. J., & Taylor, A. B. (2009). The morphology of the masticatory apparatus facilitates muscle force production at wide jaw gapes in tree-gouging common marmosets (*Callithrix jacchus*). Journal of Experimental Biology, 212(24), 4040-4055.

Ettema, G. J. C. (1996). Mechanical efficiency and efficiency of storage and release of series elastic energy in skeletal muscle during stretch–shorten cycles. *Journal of Experimental Biology*, 199(9), 1983-1997.

Gage, J. P. (1989). Mechanisms of disc displacement in the temporomandibular joint. *Australian Dental Journal*, 34(5), 427-436.

Gordon, A.M., Huxley, A.F., Julian, F.J., 1966. The variation in isometric tension with sarcomere length in vertebrate muscle fibres. J. Physiol. (Lond.) 184, 170–192.

Greaves, W. S. (1978). The jaw lever system in ungulates: A new model. *Journal of Zoology*, 184(2), 271–285.

Hansma, H. J., Langenbach, G. E. J., Koolstra, J. H., & Van Eijden, T. M. G. J. (2006). Passive resistance increases differentially in various jaw displacement directions. Journal of dentistry, 34(7), 491-497.

Horner, A. M., Azizi, E., & Roberts, T. J. (2024). The interaction of in vivo muscle operating lengths and passive stiffness in rat hindlimbs. *Journal of Experimental Biology*, 227(5). https://doi.org/10.1242/jeb.246280

Thelen, D. G. (2003). Adjustment of muscle mechanics model parameters to simulate dynamic contractions in older adults. *Journal of Biomechanical Engineering*, 125(1), 70–77.

Herrel, A., Vanhooydonck, B., & Van Damme, R. (2004). Omnivory in lacertid lizards: adaptive evolution or constraint?. *Journal of Evolutionary Biology,* 17(5), 974-984.

Herrel, A., Podos, J., Huber, S. K., & Hendry, A. P. (2005). Evolution of bite force in Darwin's finches: a key role for head width. *Journal of Evolutionary Biology,* 18(3), 669-675.

Herring, S. W. (2003). TMJ anatomy and animal models. *Journal of Musculoskeletal & Neuronal Interactions*, 3(4), 391.

Herring, S. W., Rafferty, K. L., Liu, Z. J., & Lemme, M. (2011). Mastication and the postorbital ligament: dynamic strain in soft tissues. *Integrative and Comparative Biology*, 51(2), 297-306.

Hill, A. V. (1938). The heat of shortening and the dynamic constants of muscle. *Proceedings of the Royal Society of London. Series B-Biological Sciences*, 126(843), 136–195.

Hill, A. V. (1950). The dimensions of animals and their muscular dynamics. *Science Progress*, 38(150), 209–230.

Hill, D. A., Lucas, P. W., & Cheng, P. Y. (1995). Bite forces used by Japanese macaques (*Macaca fuscata yakui*) on Yakushima Island, Japan to open aphid-induced galls on *Distylium racemosum* (Hamamelidaceae). *Journal of Zoology, 237*(1), 57–63.

Holmes, M., & Taylor, A. B. (2023). Modeling mechanical advantage from fossils: What are we missing? *American Journal of Biological Anthropology, 180*, 77.

Horner, A. M., Azizi, E., & Roberts, T. J. (2024). The interaction of in vivo muscle operating lengths and passive stiffness in rat hindlimbs. *Journal of Experimental Biology*, 227(5), jeb246280.

Hylander, W. L. (1979). The functional significance of primate mandibular form. *Journal of Morphology*, 160(2), 223–239.

Hylander, W. L. (2013). Functional links between canine height and jaw gape in catarrhines with special reference to early hominins. *American Journal of Physical Anthropology*, 150(2), 247-259.

Iriarte-Diaz, J., Terhune, C. E., Taylor, A. B., & Ross, C. F. (2017). Functional correlates of the position of the axis of rotation of the mandible during chewing in non-human primates. *Zoology*, 124, 106–118.

Iriarte-Diaz, J., Martin, A., & Laird, M.F. (In review). A reevaluation of the constrained lever model in the primate feeding system.

Kappert, K. D. R., Connesson, N., Elahi, S. A., Boonstra, S., Balm, A. J. M., van Der Heijden, F., & Payan, Y. (2021). In-vivo tongue stiffness measured by aspiration: Resting vs general anesthesia. *Journal of Biomechanics*, 114, 110147.

Konow, N., Reder, B., Bartlett, D., Jenness, D., Patel, T., Moore, J. R., & Brocklehurst, R. J. (2025). Rat superficial masseter operates at long lengths during biting. *Scientific Reports*, *15*(1), 37978.

Labeit, S., Kolmerer, B., 1995. Titins: Giant proteins in charge of muscle ultrastructure and elasticity. Science 270, 293–296.

Laird, M. F., Granatosky, M. C., Taylor, A. B., & Ross, C. F. (2020). Muscle architecture dynamics modulate performance of the superficial anterior temporalis muscle during chewing in capuchins. *Scientific Reports*, *10*(1), 6410.

Laird, M. F., Kanno, C. M., Yoakum, C. B., Fogaça, M. D., Taylor, A. B., Ross, C. F., ... & De Oliveira, J. A. (2023a). Ontogenetic changes in bite force and gape in tufted capuchins. *Journal of Experimental Biology*, 226(15), jeb245972.

Laird, M. F., Iriarte-Diaz, J., Byron, C. D., Granatosky, M. C., Taylor, A. B., & Ross, C. F. (2023b). Gape drives regional variation in temporalis architectural dynamics in tufted capuchins. *Philosophical Transactions of the Royal Society B*, *378*(1891), 20220550.

Laird, M. F., Vogel, E. R., & Pontzer, H. (2016). Chewing efficiency and occlusal functional morphology in modern humans. *Journal of Human Evolution*, 93, 1-11.

Laird, M. F., Polvadore, T. A., Hirschkorn, G. A., McKinney, J. C., Ross, C. F., Taylor, A. B., ... & Iriarte-Diaz, J. (2024). Tradeoffs between bite force and gape in *Eulemur* and *Varecia*. *Journal of Morphology*, 285(5), e21699.

Laird, M. F., Holmes, M. A., Terhune, C. E., & Taylor, A. B. (2025). A (Bite) Force to Be Reckoned With. *American Journal of Biological Anthropology*, *188*(2), e70144.

Langenbach, G. E. J., & Hannam, A. G. (1999). The role of passive muscle tensions in a three-dimensional dynamic model of the human jaw. *Archives of Oral Biology*, 44(7), 557-573.

Lazarides, E., 1980. Intermediate filaments as mechanical integrators of cellular space. Nature (London) 283, 249–256.

Lenth, R. V. (2023). *emmeans: Estimated Marginal Means, aka Least-Squares Means*. R package version 1.8.8. https://CRAN.R-project.org/package=emmeans.

Lieber, R. L., Wang, Z., Binder-Markey, B. I., Persad, L. S., Shin, A. Y., & Kaufman, K. R. (2025). Modeling implications of the relationship between active and passive skeletal muscle mechanical properties. *Journal of Biomechanics*, 178, 112423.

Manfredini, D. (2009). Etiopathogenesis of disk displacement of the temporomandibular joint: a review of the mechanisms. *Indian Journal of Dental Research*, 20(2), 212-221.

McManus, J. J. (1970). Behavior of captive opossums, *Didelphis marsupialis virginiana*. *American Midland Naturalist*, 144-169.

Miller, A. J. (1991). Craniomandibular muscles: their role in function and form. CRC Press.

Mahto, A. (2019). Splitstackshape: stack and reshape datasets after splitting concatenated values. R package version 1.4. 8.

Otten, E. (1987). A myocybernetic model of the jaw system of the rat. *Journal of Neuroscience Methods*, 21, 287–302. https://doi.org/10.1016/0165-0270(87)90123-3

Panagiotopoulou, O., Robinson, D., Iriarte-Diaz, J., Ackland, D., Taylor, A. B., & Ross, C. F. (2023). Dynamic finite element modelling of the macaque mandible during a complete mastication gape cycle. *Philosophical Transactions of the Royal Society B*, *378*(1891), 20220549.

Pereira, T. D., Tabris, N., Matsliah, A., Turner, D. M., Li, J., Ravindranath, S., ... & Murthy, M. (2022). SLEAP: A deep learning system for multi-animal pose tracking. *Nature Methods*, 19(4), 486-495.

Peterson, M. D., Pistilli, E., Haff, G. G., Hoffman, E. P., & Gordon, P. M. (2011). Progression of volume load and muscular adaptation during resistance exercise. *European Journal of Applied Physiology*, 111, 1063–1071.

Plavcan, J. M., & van Schaik, C. P. (1992). Intrasexual competition and canine dimorphism in anthropoid primates. *American Journal of Physical Anthropology*, 87(4), 461-477.

Purslow , P. P. (2020). The structure and role of intramuscular connective tissue in muscle function. Front. Physiol. 11, 495. https://doi.org/10.3389/fphys.2020.00495

R Core Team. (2023). *R: A language and environment for statistical computing*. R Foundation for Statistical Computing, Vienna, Austria. https://www.R-project.org/

Rockenfeller, R., & Günther, M. (2017). How to model a muscle's active force–length relation: A comparative study. Computer Methods in Applied Mechanics and Engineering, 313, 321–336.

Rugh, J. D., Drago, C. J., & Barghi, N. (1980). Comparison of electromyographic and phonetic measurements of vertical rest position. *The Journal of Prosthetic Dentistry*, 44(4), 450.

Ryan, J. A., Ulrich, J. M., Thielen, W., Teetor, P., Bronder, S., & Ulrich, M. J. M. (2020). Package 'quantmod'. pdf] Available at: https://cran. r-project. org/web/packages/quantmod/quantmod. pdf [Last accessed 15/02/2021].

Sivasubramani, S. M., Pandyan, D. A., Chinnasamy, R., & Kumar Kuppusamy, S. (2019). Comparison of bite force after administration of midazolam and dexmedetomidine for conscious sedation in minor oral surgery. Journal of Pharmacy and Bioallied Sciences, 11(Suppl 2), S446-S449.

Taylor, A. B., Terhune, C. E., Toler, M., Holmes, M., Ross, C. F., & Vinyard, C. J. (2018). Jaw-Muscle Fiber Architecture and Leverage in the Hard-Object Feeding Sooty Mangabey are not

Structured to Facilitate Relatively Large Bite Forces Compared to Other Papionins. The Anatomical Record, 301(2), 325–342.

Taylor, A. B., Terhune, C. E., & Vinyard, C. J. (2019). The influence of masseter and temporalis sarcomere length operating ranges as determined by laser diffraction on architectural estimates of muscle force and excursion in macaques (*Macaca fascicularis* and *Macaca mulatta*). *Archives of Oral Biology*, 105, 35-45.

Taylor, A. B., Terhune, C. E., Ross, C. F., & Vinyard, C. J. (2024). Jaw-muscle fiber architecture and skull form facilitate relatively wide jaw gapes in male cercopithecoid monkeys. *Journal of Human Evolution*, 197, 103601.

Terhune, C. E. (2013). Dietary correlates of temporomandibular joint morphology in the great apes. *American Journal of Physical Anthropology*, 150(2), 260-272.

Terhune, C. E., Hylander, W. L., Vinyard, C. J., & Taylor, A. B. (2015). Jaw-muscle architecture and mandibular morphology influence relative maximum jaw gapes in the sexually dimorphic Macaca fascicularis. *Journal of Human Evolution*, *82*, 145-158.

Terhune, C. E., Mitchell, D. R., Cooke, S. B., Kirchhoff, C. A., & Massey, J. S. (2022). Temporomandibular joint shape in anthropoid primates varies widely and is patterned by size and phylogeny. *The Anatomical Record*, *305*(9), 2227-2248.

Thelen, D. G. (2003). Adjustment of muscle mechanics model parameters to simulate dynamic contractions in older adults. *Journal of Biomechanical Engineering*, 125(1), 70–77.

Thexton, A. J., & Hiiemae, K. M. (1975). The twitch-contraction characteristics of opossum jaw musculature. *Archives of Oral Biology*, 20(11), 743-748.

Van Casteren, A., Codd, J. R., Kupczik, K., Plasqui, G., Sellers, W. I., & Henry, A. G. (2022). The cost of chewing: The energetics and evolutionary significance of mastication in humans. *Science Advances*, 8(33), eabn8351.

van Eijden, T. M. G. J., Turkawski, S. J. J., van Ruijven, L. J., & Brugman, P. (2002). Passive force characteristics of an architecturally complex muscle. *Journal of Biomechanics*, 35(9), 1183–1189. https://doi.org/10.1016/S0021-9290(02)00087-8

Verwaijen, D., Van Damme, R., & Herrel, A. (2002). Relationships between head size, bite force, prey handling efficiency and diet in two sympatric lacertid lizards. *Functional Ecology*, 16(6), 842-850.

Wall, C. E., Hanna, J. B., O'Neill, M. C., Toler, M., & Laird, M. F. (2023). Energetic costs of feeding in 12 species of small-bodied primates. *Philosophical Transactions of the Royal Society B*, 378(1891), 20220553.

Ward, S. R., Winters, T. M., O'Connor, S. M., & Lieber, R. L. (2020). Non-linear scaling of passive mechanical properties in fibers, bundles, fascicles and whole rabbit muscles. *Frontiers in Physiology*, 11, 211.

Winters, T. M., Takahashi, M., Lieber, R. L., & Ward, S. R. (2011). Whole muscle length-tension relationships are accurately modeled as scaled sarcomeres in rabbit hindlimb muscles. *Journal of Biomechanics*, 44(1), 109-115.

Yemm, R. (1976). The role of tissue elasticity in the control of mandibular resting posture. Mastication.

Zajac, F. E. (1989). Muscle and tendon: properties, models, scaling, and application to biomechanics and motor control. *Critical Reviews in Biomedical Engineering*, 17, 359–410.

Figures and Tables

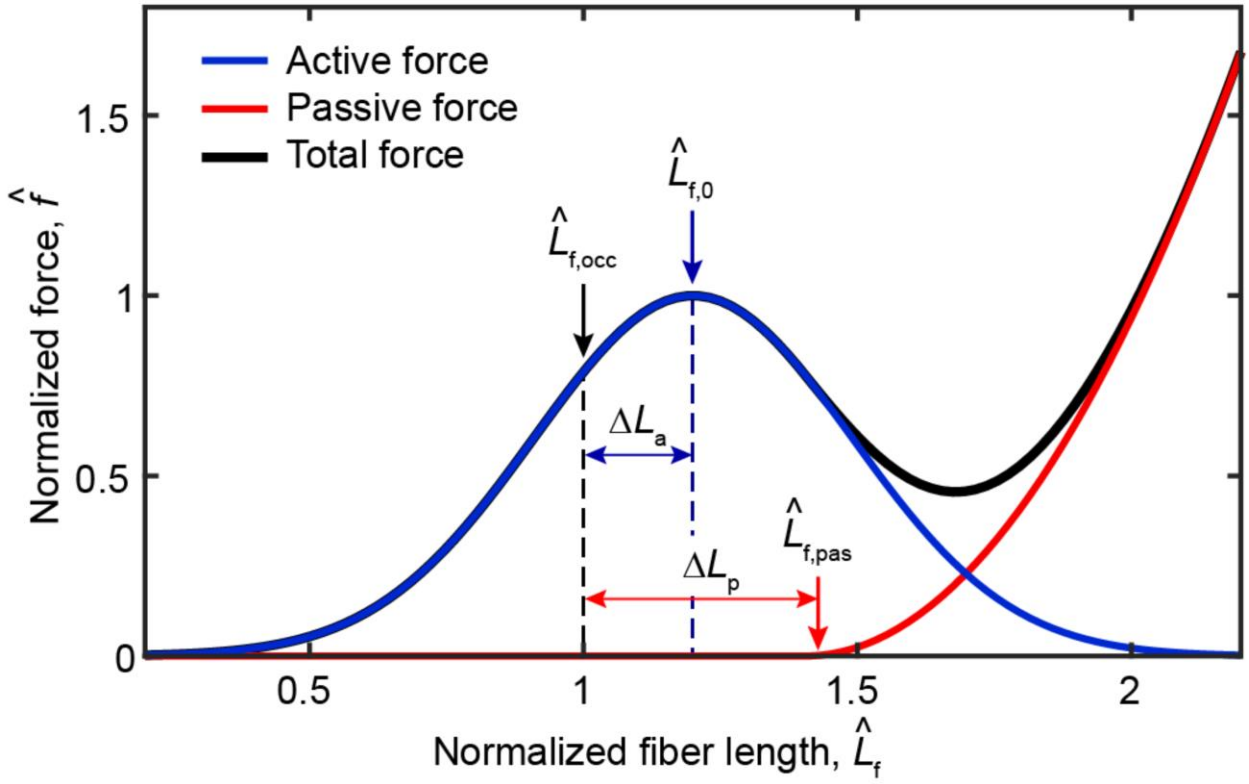

Fig. 1. A theoretical muscle force-length curve. Fiber length is normalized to $\hat{L}_{f,occ}$, the fiber length at occlusion. Active force, solid blue line, increases until the fiber reaches an optimum length, $\hat{L}_{f,0}$, after which active tension decreases. Passive force exponentially increases after it reaches the slack length, $\hat{L}_{f,pas}$. ΔL_a and ΔL_p are the active and passive offset parameters, respectively, that indicate the difference in normalized fiber length.

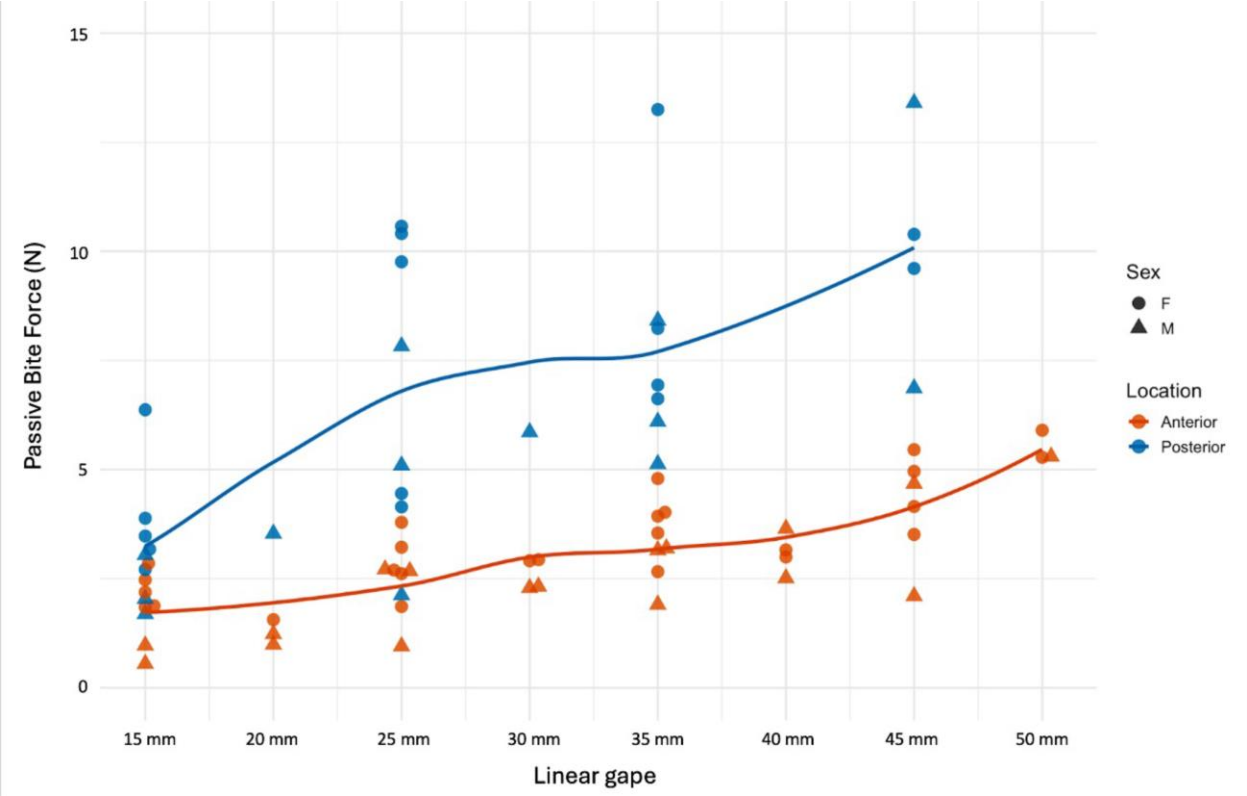

Fig. 2. LOESS curves of passive bite forces across a range of linear gapes at anterior (I1; orange) and posterior (M1; blue) bite points for males (triangles) and females (circles).

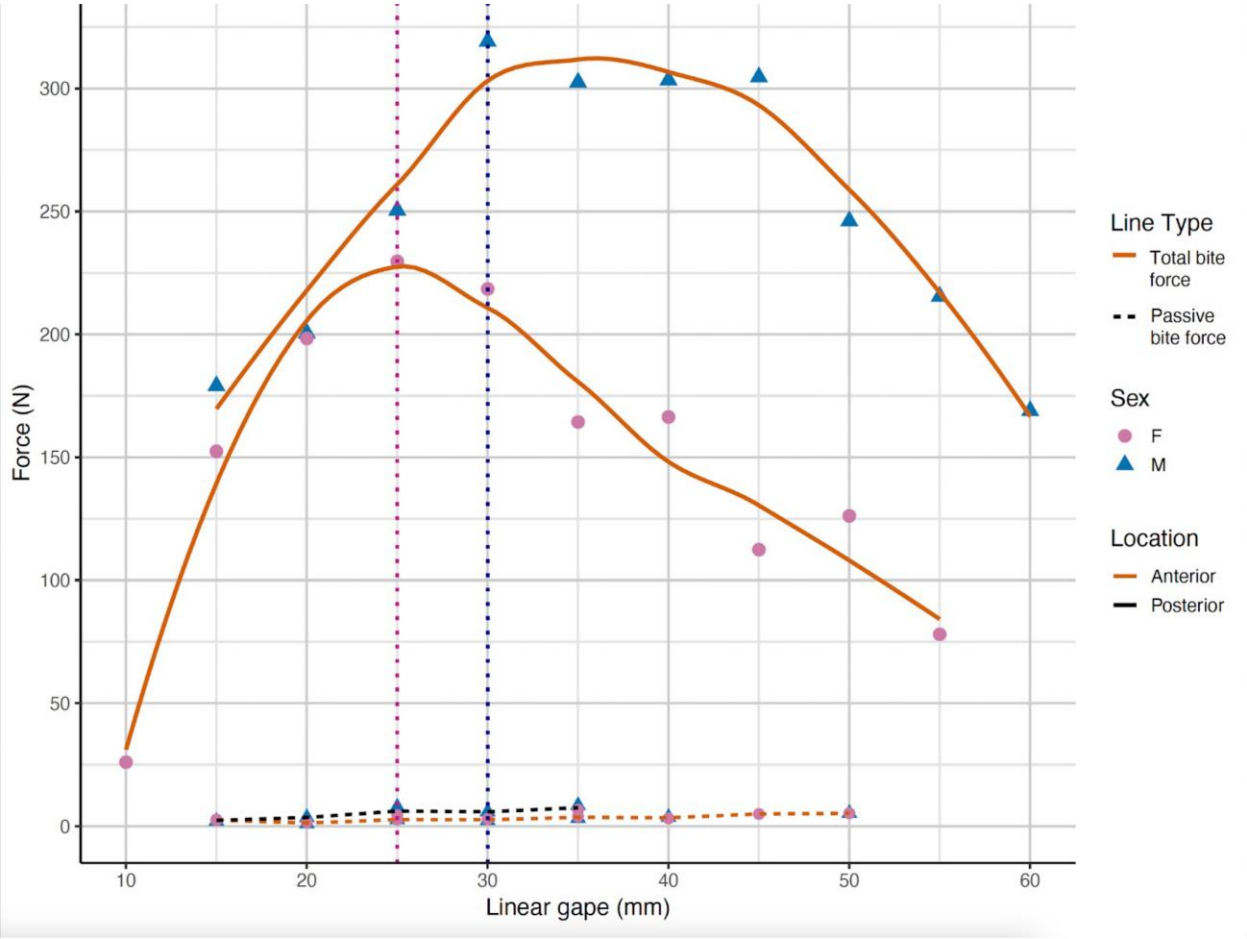

Fig. 3. Total and passive bite force data. Maximum total forces (LOESS dashed lines) come from two animals (HK-Male and LL-Female) and the maximum passive forces (solid lines) reflect data from eight macaques. Males are blue triangles and females are reddish-purple circles. Two vertical dashed lines represent maximum total bite forces for LL (left; pink) and HK (right; blue).

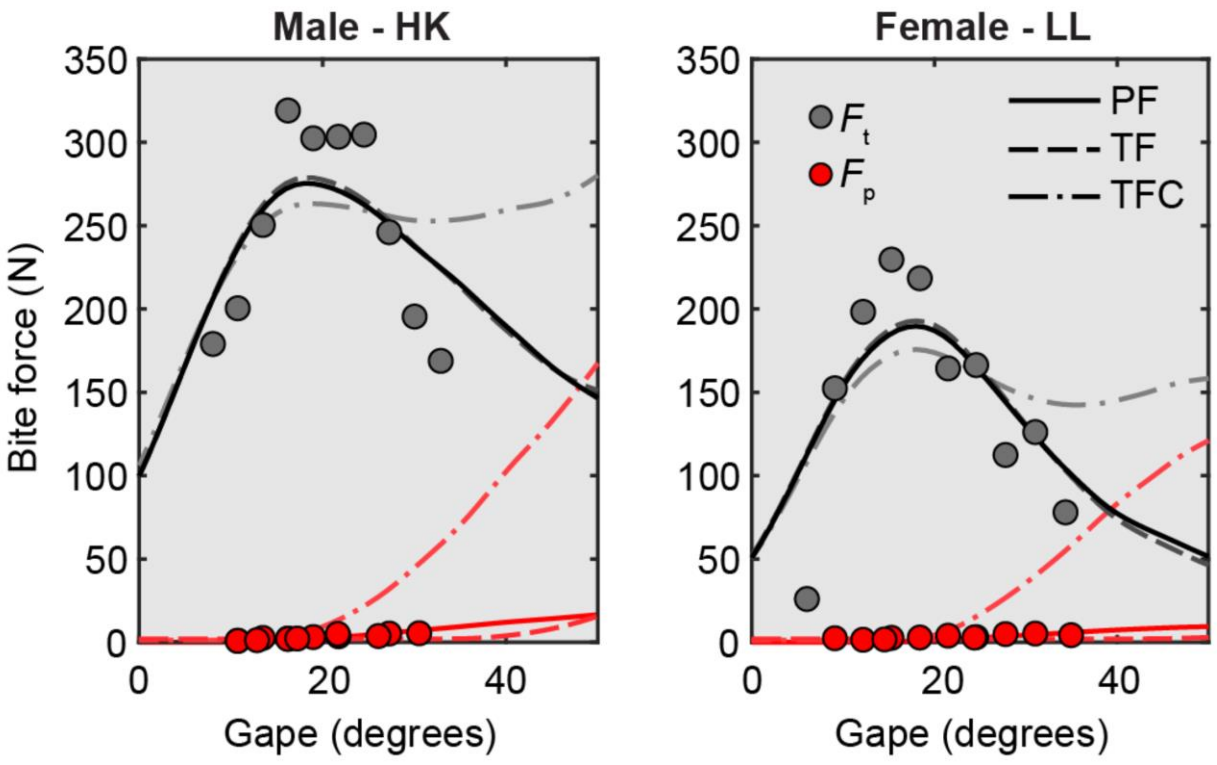

Fig. 4. Comparison of experimentally collected data on HK (male) and LL (female) with predictions from different muscle models. Gray circles are total bite force data (F_t) collected on HK and LL while awake and red circles are bite forces collected on anesthetized animals, representing passive bite forces (F_p). Three different models were fitted to the experimental data: (1) `Passive First' (PF), where passive force parameters were optimized first using experimental passive bite force data, and then these parameters were used to optimize the active force parameters; (2) `Total Force' (TF), where both passive and active force parameters were optimized together using the total bite force data only; and (3)`Total Force Constrained' (TFC), where both passive and active force components were optimized together with total bite force data only, but ΔL_a and ΔL_p are constrained to have the same value.

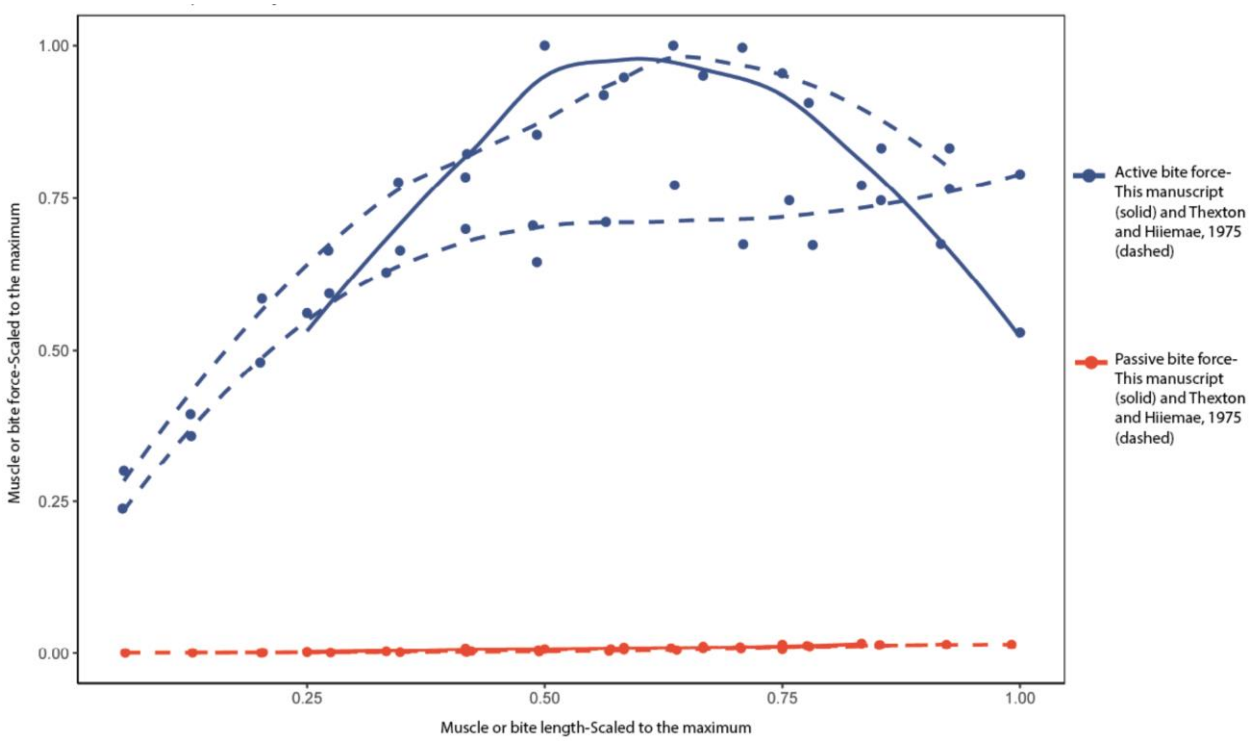

Fig. 5. Data from this manuscript of active and passive bite forces at the occlusal surface in *Macaca mulatta* and active and passive temporalis muscle forces in *Didelphis virginiana* (Thexton and Hiiemae, 1975). The passive data from Thexton and Hiiemae (1975) was originally scaled by 100. After unscaling the passive data Thexton and Hiiemae (1975), both the active and passive force data from both taxa were scaled to their respective active maxima making them directly comparable.

Table 1. Morphological measurements for each animal. Incisor overlap scores and adjusted gape follow Hylander (2013).

ID	Sex	Body Mass (kg)	Eye width (mm)	Incisor overlap (mm)	Jaw length: Condyle to I_1 (mm)	Maximum gape at the incisors (mm)	Adjusted maximum gape (mm)
FZ	M	14.6	59.06	Tip to tip	115.73	63.04	63.04
HK	M	8.8	60.05	Open: 2.2	109.11	62.1	59.9
TM	M	14.2	59.12	Tip to tip	105.18	74.59	74.59
HD	F	6.2	54.77	Open: 1.85	87.5	46.3	44.45
HP	F	8.2	49.73	Tip to tip	89.92	44.14	44.14
LL	F	8.6	52.56	Open: 2.49	96.56	54.18	51.69
RT	F	7.1	51.63	Tip to tip	93.06	51.72	51.72
SR	F	5.4	50.17	Tip to tip	76.17	49.97	49.97

Table 2. Muscle architecture data from Taylor et al., (2018) used in the models.

	Jaw length	Superficial masseter			Temporalis		
	L_j (mm)	NL_f (mm)	PCSA (cm^2)	α (degrees)	NL_f (mm)	PCSA (cm^2)	α (degrees)
Female	83.59	13.08	5.11	15.42	16.52	11.76	13.02
Male	103.56	15.98	6.69	12.19	28.48	13.92	6.23

L_j, jaw length; NL_f, normalized fiber length; PCSA, physiological cross-sectional area; α, pennation angle.

Table 3. Passive bite force data.

Location	Linear gape (mm)	Female data (range; average)[1]	Male data (range; average)[1]
Anterior	15	*n* = 5 (1.850 – 2.851N; 2.249N)	*n* = 2 (0.550 – 0.971N; 0.760N)
Anterior	20	*n* = 1 (1.561N)	*n* = 3 (0.887 – 1.234N; 1.037N)
Anterior	25	*n* = 5 (1.862 – 3.790N; 2.837N)	*n* = 3 (0.952 – 2.713N; 2.113N)
Anterior	30	*n* = 2 (2.911 – 2.935N; 2.923N)	*n* = 3 (2.042 – 2.321N; 2.217N)
Anterior	35	*n* = 5 (2.660 – 4.795N; 3.791N)	*n* = 3 (1.907 – 3.196N; 2.752N)
Anterior	40	*n* = 2 (2.997 and 3.159N; 3.078N)	*n* = 2 (2.512 and 3.645N; 3.079N)
Anterior	45	*n* = 4 (3.514 – 5.455N; 4.521N)	*n* = 2 (2.101 and 4.678N; 3.389N)
Anterior	50	*n* = 2 (5.280 and 5.901N; 5.590N)	*n* = 1 (5.298N)
Posterior	15	*n* = 5 (2.711 – 6.370N; 3.923N)	*n* = 3 (1.692 – 3.044N; 2.258N)
Posterior	20	-	*n* = 1 (3.534N)
Posterior	25	*n* = 5 (4.145 – 10.575N; 7.868N)	*n* = 3 (2.124 – 7.826N; 5.015N)
Posterior	30	-	*n* = 1 (5.85N)
Posterior	35	*n* = 4 (6.623 – 13.249N; 8.761N)	*n* = 3 (5.128 – 8.415N; 6.547N)
Posterior	40	-	-
Posterior	45	*n* = 2 (9.608 and 10.389N; 9.998N)	*n* = 2 (6.864 and 13.401N; 10.132N)

[1]*n* = number of successful data points; may include multiple data points from the same animal.

Table 4. Maximum total bite force data at each linear gape for animals LL and HK.

Linear gape (mm)	Number of bites (LL; Female)	Maximum bite force (LL; N)	Number of bites (HK; Male)	Maximum bite force (HK; N)
10	*n* = 1	26.03	*n* = 0	NA
15	*n* = 5	152.44	*n* = 1	179.06
20	*n* = 37	198.33	*n* = 41	200.47
25	*n* = 11	229.69	*n* = 25	250.43
30	*n* = 11	218.46	*n* = 59	319.14
35	*n* = 14	164.38	*n* = 59	302.48
40	*n* = 14	166.39	*n* = 35	303.40
45	*n* = 2	112.45	*n* = 28	304.64
50	*n* = 10	126.18	*n* = 40	246.12
55	*n* = 3	78.03	*n* = 22	215.42
60	*n* = 0	NA	*n* = 1	168.91

Table 5. Optimized passive and active parameters for the three modeled muscle conditions

		Passive Force					Total Force					Total Force Constrained				
		Passive		Active			Passive		Active			Passive		Active		
ID	Sex	ΔL_p	cf_p	ΔL_a	cf_a	R^2	ΔL_p	cf_p	ΔL_a	cf_a	R^2	ΔL_p	cf_p	ΔL_a	cf_a	R^2
HK	M	0.24	0.09	0.47	1.60	0.58	1.17	1.63	0.48	1.63	0.61	0.44	1.47	0.44	1.47	0.31
LL	F	0.31	0.06	0.51	1.27	0.64	1.38	1.29	0.52	1.29	0.64	0.50	1.16	0.50	1.16	0.46

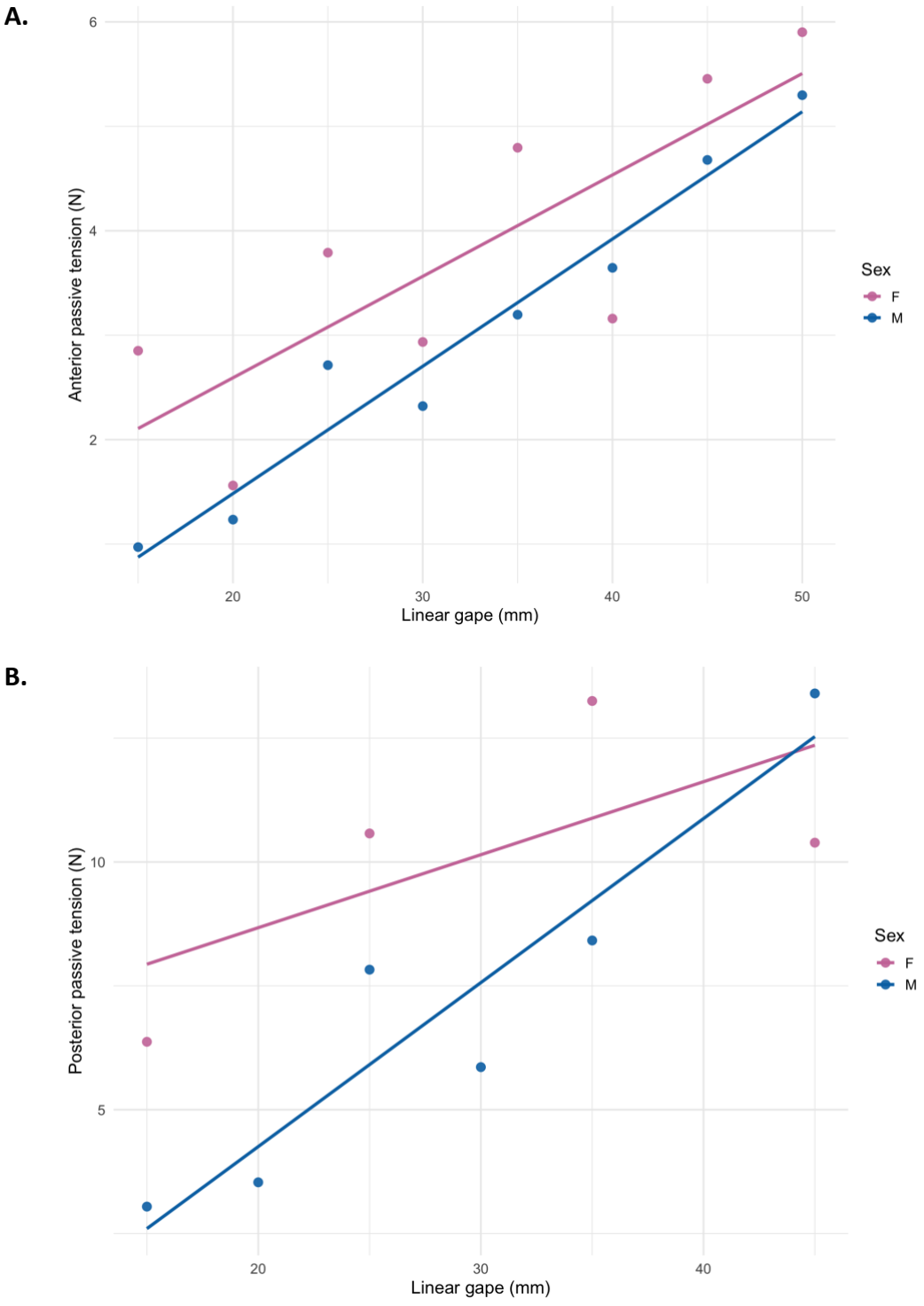

Fig. S1. Differences in maximum passive forces between males and females at I_1 (**A**) and M_1 (**B**). Females had significantly higher passive forces in anterior bite points for all gapes.

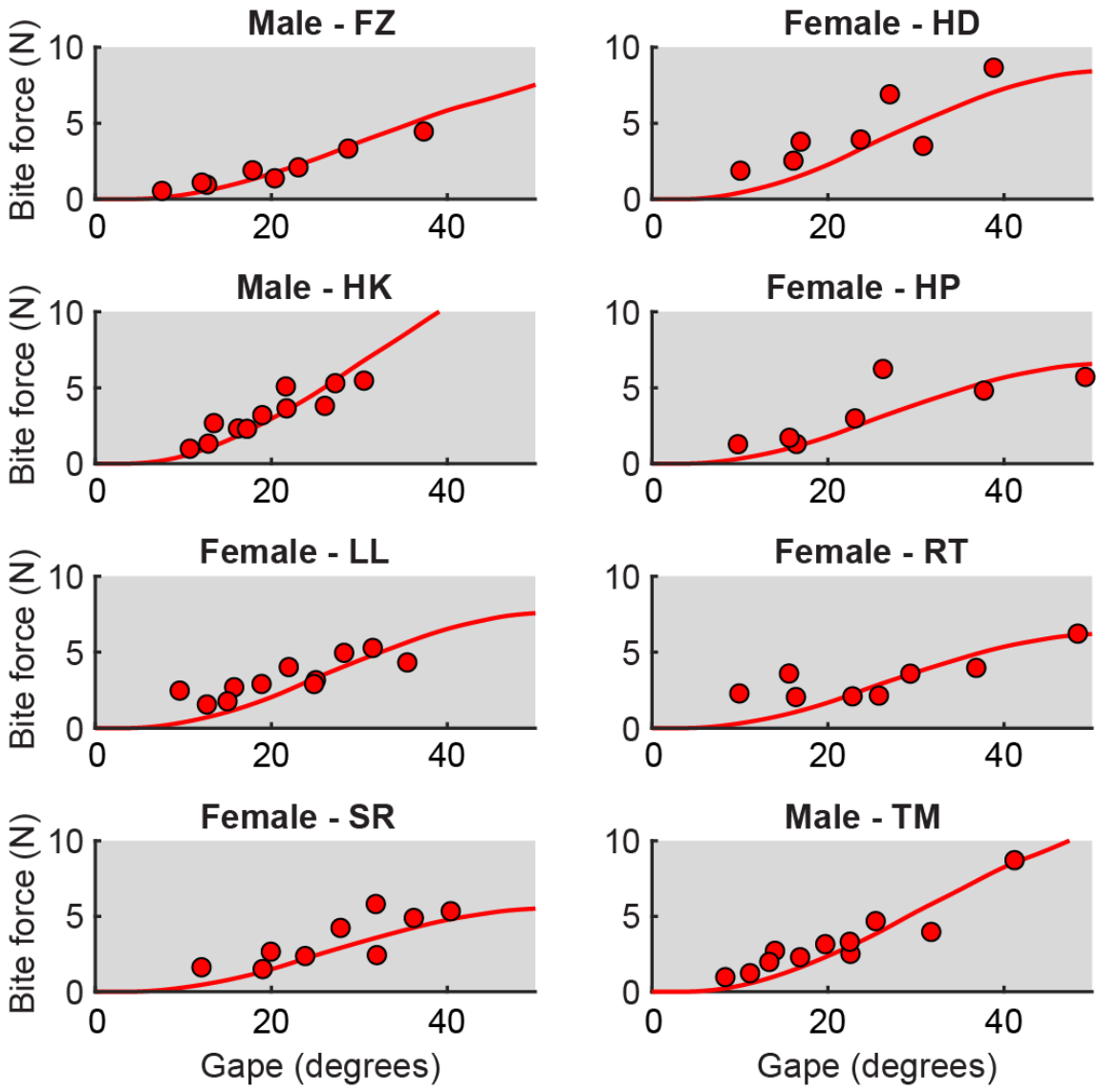

Fig. S2. Comparison of experimentally collected passive bite force data on eight anesthetized individuals. The red line shows the predicted passive bite force data for a given gape angle from muscle models optimized for each individual.

Table S1. Mechanical and physical properties of walnut and brazil nut shells.

Food type	*n*	Maximum length (average; mm)	Maximum breadth (average; mm)	Minimum breadth (average; mm)	Force-to-fracture (average; N)[1]
Brazil nut	6	46.75	22.68	12.23	614.46
Walnut	6	35.13	33.10	31.08	233.39

[1]Force-to-fracture data from Laird et al. (2023)

Table S2. Location of catastrophic fracture of shelled nuts by LL and HK.

Monkey ID	Sex	Nut type	Food #	Location of initial bite	Location of fracture
HK	M	Brazil nut	1	posterior	posterior
HK	M	Brazil nut	2	anterior	anterior
HK	M	Brazil nut	3	anterior	posterior
HK	M	Brazil nut	4	anterior	posterior
HK	M	Brazil nut	5	anterior	anterior
LL	F	Brazil nut	1	posterior	posterior
LL	F	Brazil nut	2	posterior	posterior
LL	F	Brazil nut	3	anterior	posterior
LL	F	Brazil nut	4	posterior	posterior
HK	M	Walnut	1	anterior	anterior
HK	M	Walnut	2	anterior	posterior
HK	M	Walnut	3	anterior	anterior
HK	M	Walnut	4	anterior	anterior
HK	M	Walnut	5	anterior	anterior
HK	M	Walnut	6	anterior	anterior

LL	F	Walnut	X	Attempted to fracture (briefly pouched); discarded.	
LL	F	Walnut	X	Attempted to fracture (briefly pouched); discarded.	
LL	F	Walnut	1	posterior	posterior
LL	F	Walnut	2	posterior	posterior
LL	F	Walnut	X	Attempted to fracture (briefly pouched); discarded.	
LL	F	Walnut	3	posterior	posterior
LL	F	Walnut	4	posterior	posterior

[1]Catastrophic fractures were easily observable whereas the initial microfractures were not consistently observable (on the food item) or audible (due to the noise by other macaques in the room).

Table S3. Results from LME models testing differences between passive forces measured on the anterior and posterior dentition, and between males and females on the anterior and position dentition.

All individuals-Linear gape-Anterior and Posterior					
	Estimate	**Std. Error**	**df**	**t value**	**p.value**
(Intercept)	0.21491	0.75001	49.28609	0.287	0.776
LinearGape	0.08846	0.01996	61.38592	4.431	3.94E-05
LocationPosterior	-0.05405	1.01468	61.41321	-0.053	0.958
LinearGape:Location Posterior	0.14214	0.03339	62.04977	4.257	7.13E-05
contrast	estimate	SE	df	t.ratio	p.value
Anterior-Posterior	-4.17	0.356	62.3	-11.706	<.0001
All individuals-Angular gape-Anterior and Posterior					
	Estimate	**Std. Error**	**df**	**t value**	**p.value**
(Intercept)	0.37725	0.685	46.36551	0.551	0.584
LinearGape	0.06904	0.01514	65.86135	4.561	2.27E-05
LocationPosterior	0.15172	0.96236	62.66896	0.158	0.875
LinearGape:Location	0.11624	0.02684	63.93886	4.331	5.34E-05

Posterior					
contrast	estimate	SE	df	t.ratio	p.value
Anterior-Posterior	-4.28	0.37	62.7	-11.571	<.0001
Passive forces-Linear gape-Anterior only					
	Estimate	**Std. Error**	**df**	**t value**	**p.value**
(Intercept)	0.77542	0.41803	36.54481	1.855	0.0717
LinearGape	0.08132	0.01184	34.43693	6.871	6.11E-08
SexM	-1.50633	0.69527	36.89506	-2.167	0.0368
LinearGape:SexM	0.01787	0.01976	33.6759	0.904	0.3724
contrast	estimate	SE	df	t.ratio	p.value
F-M	0.948	0.33	5.58	2.874	0.0307
Passive forces-Angular gape-Anterior only					
	Estimate	**Std. Error**	**df**	**t value**	**p.value**
(Intercept)	1.018279	0.367189	29.30161	2.773	0.00956
LinearGape	0.056762	0.007842	38.86831	7.238	1.03E-08

SexM	-1.72906	0.634353	34.46259	-2.726	0.01001
LinearGape:SexM	0.035582	0.015844	35.21285	2.246	0.03109
contrast	estimate	SE	df	t.ratio	p.value
F-M	0.376	0.317	5.87	1.184	0.2822
Passive forces-Linear gape-Posterior only					
	Estimate	**Std. Error**	**df**	**t value**	**p.value**
(Intercept)	1.41292	1.56399	24.91397	0.903	0.374961
LinearGape	0.21456	0.05126	20.92949	4.186	0.000419
SexM	-3.20662	2.42353	24.62706	-1.323	0.197951
LinearGape:SexM	0.04248	0.07611	20.34013	0.558	0.582878
contrast	estimate	SE	df	t.ratio	p.value
F-M	2.04	1.24	5.47	1.651	0.154
Passive forces- Angular gape-Posterior only					
	Estimate	**Std. Error**	**df**	**t value**	**p.value**
(Intercept)	2.02824	1.55555	24.25873	1.304	0.204515

angulargape	0.15328	0.04009	21.42948	3.824	0.000961
SexM	-3.85587	2.43064	23.93128	-1.586	0.125784
angulargape:SexM	0.09023	0.06616	20.32756	1.364	0.187539
contrast	estimate	SE	df	t.ratio	p.value
F-M	0.985	1.3	5.52	0.757	0.4804

Table S4. Confidence intervals for the relationships between anterior and posterior passive forces and gape.

All animals: Anterior Passive forces					
Gape	**emmean**	**SE**	**df**	**lower.CL**	**upper.CL**
15mm	1.77	0.446	1.41	**-1.156**	**4.69**
20mm	1.06	0.507	2.44	**-0.786**	**2.91**
25mm	2.5	0.438	1.33	**-0.665**	**5.66**

30mm	2.27	0.482	1.97	0.172	4.37
35mm	3.33	0.438	1.33	0.171	6.49
40mm	2.73	0.482	1.97	0.636	4.83
45mm	4.07	0.454	1.53	1.414	6.73
50mm	5.02	0.51	2.44	3.163	6.87
All animals: Posterior Passive forces					
Gape	**emmean**	**SE**	**df**	**lower.CL**	**upper.CL**
15mm	3.17	1.15	1.91	**-1.972**	**8.32**
20mm	3.64	2.49	15.98	**-1.638**	**8.91**
25mm	6.67	1.15	1.91	1.527	11.82
30mm	5.96	2.49	15.98	0.687	11.24
35mm	7.81	1.18	2.21	3.169	12.45
45mm	10.43	1.4	4.17	6.599	14.27

Table S5. Passive component parameters optimized from passive bite force data.

ID	Sex	Passive parameters		
		ΔL_p	cf_p	R^2 *adjusted*
FZ	M	0.28	0.04	0.82
HK	M	0.24	0.09	0.58
TM	M	0.28	0.08	0.74
HD	F	0.34	0.09	0.28
HP	F	0.38	0.06	0.16
LL	F	0.31	0.06	0.27
RT	F	0.37	0.05	0.31
SR	F	0.36	0.10	0.18